A Novel 3D Pseudo-spectral Analysis of Photonic Crystal Slabs

K. Varis[(a)], and A. R. Baghai-Wadji[(b)]
[(a)] Helsinki University of Technology, Optoelectronics Laboratory,
P.O. Box 3500, FIN-02015 HUT, Finland, EU
karri.varis@hut.fi
[(b)] Vienna University of Technology, E351,
Gusshausstrasse 27-29, A-1040 Vienna, Austria, EU
alireza.baghai-wadji@tuwien.ac.at

Abstract—**We consider a double-periodic slab which is characterized by two lattice vectors $\mathbf{a}_1$ and $\mathbf{a}_2$ on the $(x,y)-$plane, the thickness h_z and a three-dimensional scalar function $\varepsilon(x,y,z)$ specifying the dielectric constitution of the slab. Above and below the slab is free space. These assumptions imply that the $z-$direction is special in this problem. Therefore, following a general scheme we diagonalize the Maxwell's equations with respect to this direction. The periodicity in two directions suggests the use of spatially harmonic functions as a basis. We exploit this property; however, contrary to the traditional schemes, we propose an expansion of the fields in the form $\Psi(\mathbf{r},z)=\sum_n f_n(z)\exp(j\mathbf{k}_n\cdot\mathbf{r})$ allowing $f_n(z)$ to be a fairly general function of the z-coordinate, rather than an exponential function. In this expression r is the position vector in the $(x,y-)$ transversal plane. To guarantee maximum flexibility we discretize f in terms of finite differences. We demonstrate the superiority of our method by discussing the following properties: *i*) Diagonalization only involves the transversal field components, *ii*) Diagonalization allows us easily to construct and implement various boundary conditions at the bounding surfaces $z=0$ and $z=h_z$, *iii*) The resulting discretized system is extraordinarily stable and robust, and facilitates fast computations; from the computational performance point of view it compares well with existing methods, while it by far applies to larger class of problems, *iv*) It allows to use both the radian frequency ω and the wavevector K as input parameters. Therefore, the resulting discrete system can be solved at individual $(\omega,\mathbf{K})$-points of interest, *v*) Finally, the method is applicable to both the eigenstate end the excitation problems.**

I. Introduction

We consider a doubly-periodic slab which is characterized by a dielectric function $\varepsilon(x,y,z)$ satisfying the condition $\varepsilon\ (\mathbf{r}+m\mathbf{a}_1+n\mathbf{a}_2,z)=\varepsilon(\mathbf{r},z)$ for arbitrary negative or positive whole numbers m and n. Here $\mathbf{r}$ is the position vector and $\mathbf{a}_1$ and $\mathbf{a}_2$ are lattice vectors in the $(x,y)-$plane. Above and below the slab, which is bounded by the planes $z=0$ and $z=h_z$, various boundary conditions can be accommodated, e.g. electrically or magnetically conducting, or, dielectrically or magnetically open, or, a combination of both. In the case of open boundaries we require that the cladding media satisfy the following conditions: a) the dielectric media are independent of the $z-$coordinate; i.e. $\partial\varepsilon(x,y,z)/\partial_z\equiv 0$, and b) the media possess the same periodicity properties as in the slab along the lattice vector directions.

The periodicity property in two directions suggests the use of spatially harmonic basis functions in the transversal $(x,y)-$plane. Obviously the $z-$direction in our slab problem, suggests the diagonalization of the Maxwell's equations with respect to this ''normal'' direction. We exploit these properties and expand the fields in terms of a sum of products of separable functions in the form $\Psi=\sum_n f_n(z)\exp(j\mathbf{k}_n\cdot\mathbf{r})$. In order to determine various functions $f_n(z)$, we discretize them in terms of finite differences (FD) which leads to a simple yet powerful implementation. Standard FD techniques involve all the three components of the electric field **E** and the magnetic field **H**. On contrary, in the proposed diagonalized form only an optimized subset of field components are involved: It turns out that only those field components which enter the interface- and boundary conditions on $z=$ const planes have to included in our formalism. In the next section it is shown that, once the transversal field components $\mathbf{e}=(e_1,e_2)$ and $\mathbf{h}=(h_1,h_2)$ are known on a $z=$ const plane, the remaining components in the normal (diagonalization) direction can be derived easily, straightforwardly and inexpensively.

II. Planewave FD in 3D

A. Constructing the diagonalized operator

The curl operator can be written in the form

$$\nabla\times=\partial_x\mathbf{N}_1+\partial_y\mathbf{N}_2+\partial_z\mathbf{N}_3, \tag{1}$$

where

$$\mathbf{N}_1=\begin{bmatrix}0&0&0\\0&0&-1\\0&1&0\end{bmatrix}, \tag{2a}$$

$$\mathbf{N}_2 = \begin{bmatrix} 0 & 0 & 1 \\ 0 & 0 & 0 \\ -1 & 0 & 0 \end{bmatrix}, \tag{2b}$$

$$\mathbf{N}_3 = \begin{bmatrix} 0 & -1 & 0 \\ 1 & 0 & 0 \\ 0 & 0 & 0 \end{bmatrix}. \tag{2c}$$

Adopting this notation the Maxwell's equations are

$$(\partial_x \mathbf{N}_1 + \partial_y \mathbf{N}_2 + \partial_z \mathbf{N}_3)\,\mathbf{E} = j\omega\mu\mathbf{H}, \tag{3a}$$

$$(\partial_x \mathbf{N}_1 + \partial_y \mathbf{N}_2 + \partial_z \mathbf{N}_3)\,\mathbf{H} = -j\omega\varepsilon\mathbf{E}. \tag{3b}$$

In what follows we describe a simple recipe for the diagonalization of Maxwell's equations as written in (3). Thereby, we arbitrarily choose any of the directions x, y, or z. However, we reference to our discussion in the introduction and select the $z-$direction as our diagonalization direction. To this end, we consider the decomposition of the 3×3 identity matrix $\mathbf{I}$ in the following form

$$\mathbf{I} = \begin{bmatrix} 1 & 0 & 0 \\ 0 & 1 & 0 \\ 0 & 0 & 0 \end{bmatrix} + \begin{bmatrix} 0 & 0 & 0 \\ 0 & 0 & 0 \\ 0 & 0 & 1 \end{bmatrix} \tag{4a}$$

$$= \begin{bmatrix} 0 & 1 & 0 \\ -1 & 0 & 0 \\ 0 & 0 & 0 \end{bmatrix} \begin{bmatrix} 0 & -1 & 0 \\ 1 & 0 & 0 \\ 0 & 0 & 0 \end{bmatrix} + \underbrace{\begin{bmatrix} 0 & 0 & 0 \\ 0 & 0 & 0 \\ 0 & 0 & 1 \end{bmatrix}}_{\mathbf{U}_3} \tag{4b}$$

$$= \mathbf{N}_3^T \mathbf{N}_3 + \mathbf{U}_3, \tag{4c}$$

where the matrix $\mathbf{U}_3$ in (4b) has been introduced in the obvious manner. The superscript T denotes transposition.

Recognizing the form of $\mathbf{N}_3^T\mathbf{N}_3$ (Eqs. (4)) and the orthogonality property of $\mathbf{N}_3$ and $\mathbf{U}_3$, and thus $\mathbf{N}_3^T$ and $\mathbf{U}_3$, the diagonalization procedure amounts to the following steps: (i) Multiply (3a), from the left, successively by $\mathbf{N}_3^T$ and $\mathbf{U}_3$, (ii) multiply (3b), from the left, successively by $\mathbf{N}_3^T$ and $\mathbf{U}_3$. (iii) It is immediately seen that the equations obtained from the $\mathbf{U}_3-$multiplication allow us to express the transversal field components e_1, e_2, h_1 and h_2 in terms of the normal field components e_3, h_3. Furthermore, it can be seen that these equations do not involve any $z-$derivatives at all. Substituting the resulting matrix equation in the combined systems of equations, obtained from the multiplication of $\mathbf{N}_3^T$, results in the desired diagonalized form. In the following we provide examples by discussing several special cases.

In the present case, considering isotropic media only, the equations (3) are extraordinarily simple: Once the equations are written out explicitly the reader can easily recognize all the aforementioned relationships just simply by inspection. We have

$$\partial_x \begin{bmatrix} 0 \\ -e_3 \\ e_2 \end{bmatrix} + \partial_y \begin{bmatrix} e_3 \\ 0 \\ -e_1 \end{bmatrix} - j\omega\mu \begin{bmatrix} h_1 \\ h_2 \\ h_3 \end{bmatrix} = -\partial_z \begin{bmatrix} -e_2 \\ e_1 \\ 0 \end{bmatrix}, \tag{5a}$$

$$\partial_x \begin{bmatrix} 0 \\ -h_3 \\ h_2 \end{bmatrix} + \partial_y \begin{bmatrix} h_3 \\ 0 \\ -h_1 \end{bmatrix} + j\omega\varepsilon \begin{bmatrix} e_1 \\ e_2 \\ e_3 \end{bmatrix} = -\partial_z \begin{bmatrix} -h_2 \\ h_1 \\ 0 \end{bmatrix}. \tag{5b}$$

Due to the properties of the Maxwell's equations, (5b) can be obtained from (5a) simply by the replacements $h_i \leftrightarrow e_i$ $(i = 1,2,3)$ and $\varepsilon \leftrightarrow -\mu$. Therefore, it is sufficient to restrict our manipulations only to one set of these equations. We consider (5a). Obviously these equations split into the equations

$$\partial_x \begin{bmatrix} e_3 \\ 0 \end{bmatrix} + \partial_y \begin{bmatrix} 0 \\ e_3 \end{bmatrix} + j\omega\mu \begin{bmatrix} h_2 \\ -h_1 \end{bmatrix} = \partial_z \begin{bmatrix} e_1 \\ e_2 \end{bmatrix}, \tag{6}$$

and

$$h_3 = \frac{1}{j\omega\mu}\partial_x e_2 - \frac{1}{j\omega\mu}\partial_y e_1. \tag{7}$$

The counterpart of (7) is

$$e_3 = -\frac{1}{j\omega\varepsilon}\partial_x h_2 + \frac{1}{j\omega\varepsilon}\partial_y h_1. \tag{8}$$

Substituting e_3 from (8) into (6) we obtain

$$\mathscr{A} \begin{bmatrix} h_1 \\ h_2 \end{bmatrix} = \partial_z \begin{bmatrix} e_1 \\ e_2 \end{bmatrix}, \tag{9}$$

where

$$\mathscr{A} = \begin{bmatrix} \partial_x \frac{1}{j\omega\varepsilon}\partial_y & -\partial_x \frac{1}{j\omega\varepsilon}\partial_x + j\omega\mu \\ \partial_y \frac{1}{j\omega\varepsilon}\partial_y - j\omega\mu & -\partial_y \frac{1}{j\omega\varepsilon}\partial_x \end{bmatrix}. \tag{10}$$

Performing the aforementioned replacements we obtain the corresponding counterpart

$$\mathscr{B} \begin{bmatrix} e_1 \\ e_2 \end{bmatrix} = \partial_z \begin{bmatrix} h_1 \\ h_2 \end{bmatrix}, \tag{11}$$

where

$$\mathscr{B} = \begin{bmatrix} -\partial_x \frac{1}{j\omega\mu}\partial_y & \partial_x \frac{1}{j\omega\mu}\partial_x - j\omega\varepsilon \\ -\partial_y \frac{1}{j\omega\mu}\partial_y + j\omega\varepsilon & \partial_y \frac{1}{j\omega\mu}\partial_x \end{bmatrix}. \tag{12}$$

Therefore, we have transformed the Maxwell's curl equations into the following two sets of equations

$$\begin{bmatrix} 0 & \mathscr{A} \\ \mathscr{B} & 0 \end{bmatrix} \begin{bmatrix} e_1 \\ e_2 \\ h_1 \\ h_2 \end{bmatrix} = \partial_z \begin{bmatrix} e_1 \\ e_2 \\ h_1 \\ h_2 \end{bmatrix}, \tag{13}$$

and

$$\begin{bmatrix} 0 & 0 & \frac{1}{j\omega\varepsilon}\partial_y & -\frac{1}{j\omega\varepsilon}\partial_x \\ -\frac{1}{j\omega\mu}\partial_y & \frac{1}{j\omega\mu}\partial_x & 0 & 0 \end{bmatrix} \begin{bmatrix} e_1 \\ e_2 \\ h_1 \\ h_2 \end{bmatrix} = \begin{bmatrix} e_3 \\ h_3 \end{bmatrix}. \tag{14}$$

Equation (13) is the desired diagonalized form with the aforementioned properties: This equation only involves variables which enter into the *interface conditions* if we cross a $z = z_i = \text{const}$ plane at a point (x_i, y_i, z_i) in the $z-$direction. This property implies that if we are given the field distribution on the z_i-plane, we obtain the rate of change of the field distribution in the $z-$direction by applying the matrix operator at the LHS of (13). Consequently, by having the information about the field distribution on the z_i-plane, and its rate of change we can approximate the field distribution on a neighboring plane $z = z_0 \pm \Delta$. We would like to point out that by repeated application of the matrix operator at the LHS of (13) to this equation, and using (13), we obtain higher-order derivatives of the field vector in (13). Having computed higher-order derivatives, and using Taylor series expansions we can construct approximations to the fields to any order of accuracy desired.

We wish to conclude this section with the following comment: The *Normal components* e_3 and h_3 can be computed from the transversal field distribution by using operators and material parameters which only depend on the x and y transversal coordinates as seen in (14).

B. Discretization

1) Field expansions: The periodicity in two dimensions suggests the following expansion for the fields

$$\Psi(x,y,z) = \sum_{m,n} f_{m,n}(z) e^{j\mathbf{k}_{m,n}\cdot\mathbf{r}}, \tag{15}$$

where Ψ represents any of the transversal field components and $\mathbf{r}$ is the position vector on a $z = \text{const}$ plane. The reciprocal vector $\mathbf{k}_{m,n}$ denotes a certain lattice vector superimposed by a Bloch phasing vector $\mathbf{K} = K_1\mathbf{k}_1 + K_2\mathbf{k}_2$ which can be conveniently written in the following form

$$\mathbf{k}_{m,n} = (m+K_1)\mathbf{k}_1 + (n+K_2)\mathbf{k}_2, \tag{16}$$

for a discrete $M \times N$ set of reciprocal lattice. The expansion coefficients $f_{m,n}(z)$ are generally functions of $z-$coordinate. The next section is devoted to the discretization of the fields in the $z-$direction, followed by a thorough discussion of the specifics of the numerical implementation.

The choice of the harmonic dependence in the $(x,y)-$plane has been inspired by two reasons: (*i*) operators $\mathscr{A}$ and $\mathscr{B}$ only involve derivatives with respect to x and y which can be evaluated efficiently and (*ii*) the implementation of the Bloch periodic boundaries is straightforward.

2) Discretization in the orthogonalization direction: According to our diagonalization formula, the application of the matrix operator, as defined in (10), to the transversal magnetic **h**-field on a certain plane $z = z_0 = \text{const}$, results in the normal derivative of the transversal electric **e**-field on the same plane. This property can be utilized in establishing a relationship between fields which are defined on consecutive $z = \text{const}$ layers. In this section we develop the general idea and briefly address issues concerning the accuracy of the numerical results. In the next section we will focus on procedural details.

To communicate the basic idea, we start with probably the simplest assumption: Assume that $e_2 \equiv 0$ and $h_1 \equiv 0$ and that h_2 is given on the plane $z = 0$. Our goal is to establish a relationship between e_1 on planes $z = -\Delta/2$ and $z = \Delta/2$ to h_2 on the plane $z = 0$. Using Taylor's series expansion we can write

$$e_1\left(\frac{\Delta}{2}\right) = e_1(0) + \frac{\Delta}{2}\left\{\left(\frac{\partial e_1}{\partial z}\right)(0^+)\right\} + \frac{\Delta^2}{8}\left\{\left(\frac{\partial^2 e_1}{\partial z^2}\right)(0^+)\right\} + O^3(\Delta), \tag{17a}$$

$$e_1\left(-\frac{\Delta}{2}\right) = e_1(0) - \frac{\Delta}{2}\left\{\left(\frac{\partial e_1}{\partial z}\right)(0^-)\right\} + \frac{\Delta^2}{8}\left\{\left(\frac{\partial^2 e_1}{\partial z^2}\right)(0^-)\right\} + O^3(\Delta), \tag{17b}$$

where the symbols $+$ and $-$, respectively, indicate that the $z-$derivatives have to be computed at $0+\varepsilon$ and $0-\varepsilon$ for arbitrarily small but positive ε. The derivatives can be calculated using (9) and the information about the function h_2 on the $z = 0$ plane. Subtracting (17b) from (17a), and keeping the first order terms only, we obtain

$$e_1\left(\frac{\Delta}{2}\right) - e_1\left(-\frac{\Delta}{2}\right) = \frac{\Delta}{2}\left\{\left(\frac{\partial e_1}{\partial z}\right)(0^+) + \left(\frac{\partial e_1}{\partial z}\right)(0^-)\right\}. \tag{18}$$

In view of the operator $\mathscr{A}$ in (10) we recognize that if the material parameters on the two sides of the $(z=0)-$plane are the same, the involved derivatives are equal to an arbitrary order. In present case the second order derivatives cancel out and the error term in this expression is an O^3- term in Δ. If the material parameters on the two sides of the $(z=0)-$plane are different, then they have to be averaged, leading to an accuracy of only order O^2 in Δ. Similar results can be obtained for the remaining three transversal field components.

3) Construction of the system matrix: In our formulation we have adopted the following notation: Assume a basis consisting of $M \times N$ plane waves. Let $\mathbf{e}_o$ and $\mathbf{h}_o$, respectively, be $2 \times M \times N$ coefficient vectors representing the electric and magnetic fields, which are defined on the $z = o\Delta-$plane. (Note that $M \times N$ coefficients are required for each of the $x-$ and $y-$directions.) Let the $2 \times M \times N$ by $2 \times M \times N$ sub-matrix $\widehat{\mathbf{A}}_o$, be the discrete version of $\mathscr{A}$, multiplied by Δ, and evaluated on the plane $z = o\Delta$. Similarly, let $\widehat{\mathbf{B}}_o$ represent $\mathscr{B}$. Using this notation we can establish relationships between the electric fields on the planes $o-1/2$ and $o+1/2$, and the magnetic field on the interleaved plane o. Likewise we can establish relationships between the magnetic fields on the planes o and $o+1$, and the electric field on the interleaved plane $o+1/2$. Keeping first order expansion terms only, we obtain the result given in (19),

$$\mathbf{e}_{o-\frac{1}{2}} - \mathbf{e}_{o+\frac{1}{2}} + \widehat{\mathbf{A}}_o h_o = \mathbf{0}, \tag{19a}$$

$$\mathbf{h}_o - \mathbf{h}_{o+1} + \widehat{\mathbf{B}}_{o+\frac{1}{2}} \mathbf{e}_{o+\frac{1}{2}} = \mathbf{0}. \tag{19b}$$

We recognize that the equation in (19) comprise a finite difference implementation. However, in contrast to the standard formulations, the present formulation is based on a finite difference discretization of the Fourier coefficients, rather than of the fields in the spatial domain [1].

The dielectric function characterizing the slab is defined between layers $[0, O\Delta]$, where O is the index of the last layer. Furthermore, in order to incorporate the boundary condition equations in our system of equations, we need to define the electric fields on two layers, -0.5Δ and $(O+0.5)\Delta$, outside the slab

$$\Phi_l \mathbf{e}_{0.5} - \mathbf{h}_0 = \mathbf{0}, \tag{20a}$$

$$\mathbf{h}_O + \Phi_u \mathbf{e}_{O+0.5} = \mathbf{0}. \tag{20b}$$

The following section is devoted to the construction of these equations.

The general system equation can be created by formulating equations (19) for each of the $z-$layer in the slab and incorporating the boundary conditions (20). Collecting all unknowns into one vector $\mathbf{f}$ and all multipliers into one matrix $\mathbf{M}$ leads to

$$\mathbf{M}\mathbf{f} = \mathbf{0}. \tag{21}$$

The efficient solution of this homogeneous equation will be discussed below.

C. Boundary conditions

Our goal is to interrelate the electric- and magnetic fields on the lowest- and most upper bounding planes.

Various boundary conditions can arise in the applications: In the case of electrically- or magnetically conducting boundaries, e.g. we merely need to require that the electric or the magnetic field, respectively, vanishes. In this paper we address a slightly more complex problem with mixed-type boundary conditions by assuming free space above $(z > h_z)$ and beneath $(z < 0)$ our slab. Generally speaking our formulation is valid whenever the following conditions are met: (i) $\partial\varepsilon(x,y,z)/\partial_z \equiv 0$ for $z < 0$ and $z > h_z$. (Material is homogeneous in the z-direction). (ii) The materials above and below the slab share the lattice periodicity with the slab.

These conditions suggest slightly different field expansions for the fields in regions outside the slab:

$$\Psi(x,y,z) = \sum_{m,n,o} \alpha_o f_{m,n,o} e^{\lambda_o z} e^{j\mathbf{k}_{m,n}\cdot\mathbf{r}}. \tag{22}$$

Here λ_o represents the complex-valued propagation constant in $z-$direction associated with one of the $4 \times M \times N$ eigenvectors, and $f_{m,n,o}$ is the corresponding coefficient. Substituting (22) into (13) and utilizing the orthogonal property of the basis functions involved results in the eigenvalue equation in (23),

$$\begin{bmatrix} 0 & \mathscr{A} \\ \mathscr{B} & 0 \end{bmatrix} \begin{bmatrix} \mathbf{e} \\ \mathbf{h} \end{bmatrix} = \lambda \begin{bmatrix} \mathbf{e} \\ \mathbf{h} \end{bmatrix}. \tag{23}$$

For ε varying in the (x,y)-plane, we need to solve the system numerically for $4 \times M \times N$ eigenpairs. Restricting ourselves to constant ε, the general $4 \times M \times N$ eigenvalue system decouples into $M \times N$ (analytically solvable) eigenvalue systems of dimension 4. For constant ε, the system has two doubly degenerate eigenvalues for each $[m,n]$ pair

$$\lambda_{m,n} = \pm w_{m,n} = \pm\sqrt{d_x^2(m,n) + d_y^2(m,n) - \omega^2\varepsilon\mu}, \tag{24}$$

where w is the magnitude of the eigenvalue. The symbol $d_x(m,n)$ is related to the numerical value of the basis function derivative as defined in (25).

$$\frac{\partial}{\partial x} e^{j\mathbf{k}_{n,m}\cdot\mathbf{r}} = j d_x(m,n) e^{j\mathbf{k}_{n,m}\cdot\mathbf{r}} \tag{25}$$

A similar definition holds for $d_y(m,n)$. These values depend on the reciprocal lattice geometry and will considered in more detail later.

The corresponding eigenvectors can also be solved analytically, which are summarized below

$$\Psi^1_{-w} = \begin{bmatrix} -j\frac{d_x d_y}{w\omega\varepsilon} \\ -j\frac{d_y^2-\omega^2\varepsilon\mu}{w\omega\varepsilon} \\ 1 \\ 0 \end{bmatrix}, \quad \Psi^2_{-w} = \begin{bmatrix} j\frac{d_x^2-\omega^2\varepsilon\mu}{w\omega\varepsilon} \\ j\frac{d_x d_y}{w\omega\varepsilon} \\ 0 \\ 1 \end{bmatrix}, \tag{26a}$$

$$\Psi^1_{w} = \begin{bmatrix} -j\frac{d_x d_y}{w\omega\varepsilon} \\ -j\frac{d_y^2-\omega^2\varepsilon\mu}{w\omega\varepsilon} \\ -1 \\ 0 \end{bmatrix}, \quad \Psi^2_{w} = \begin{bmatrix} j\frac{d_x^2-\omega^2\varepsilon\mu}{w\omega\varepsilon} \\ j\frac{d_x d_y}{w\omega\varepsilon} \\ 0 \\ -1 \end{bmatrix}. \tag{26b}$$

Since eigenvectors are known up to a constant multiplier the normalization of the eigenvectors is arbitrary. Here we have chosen a multiplier which produces a h-field with unity length as depicted in (20).

A few remarks are in place: *i*) If w becomes complex-valued for any m,n pair, then the corresponding eigenmode radiates energy away from the slab into infinity, preventing the formation of bounded modes. *ii*) For $z > h_z$ we have to discard half of the eigenvectors which correspond to positive eigenvalues in order to satisfy the Sommerfeld's radiation condition (Inclusion of the fields with finite energy.). Similarly we have to discard eigenvectors corresponding to $\lambda < 0$ in the $z < 0$ region.

Finally, it should be pointed out that in our finite difference implementation we have defined the e-fields at discrete $z = (o+0.5)\Delta-$layers, while the $h-$ fields have been defined at $z = o\Delta-$layers. We should be aware of this fact whenever a shift of the fields by a distance 0.5Δ becomes necessary, e.g. in establishing a relationship between the field components. In present case this relationship can be established fairly easily since we know the z-directional propagation constant of the eigenvectors.

Taking into account these details we obtain the matrices which describe the boundary conditions

$$\Phi_{l,u}(m,n) = \frac{e^{0.5\Delta w_{l,u}(m,n)}}{j w_{l,u}(m,n)\omega\varepsilon_{l,u}} \times \begin{bmatrix} d_x(m,n)d_y(m,n) & -d_x^2(m,n)+\omega^2\varepsilon_{l,u}\mu \\ d_y^2(m,n)-\omega^2\varepsilon_{l,u}\mu & -d_x(m,n)d_y(m,n) \end{bmatrix} \tag{27}$$

Here the subindices l and u, respectively, indicate the lower and the upper semispaces. We can obtain discretized versions of this equation by replacing the matrix entries by diagonal submatrices, whose elements individually correspond to different (m,n)-pairs. For semispaces with non-constant ε, these submatrices will become dense since the eigenvectors of (23) will in general have $4\times M\times N$ non-zero elements.

D. Solving the equation system

Ordinarily system matrices for three dimensional problems can be prohibitively large. Therefore, we recommend the use of iterative solvers. Most solvers operate only on matrix vector products which frees us from constructing the matrix; only a routine constructing vector products is needed. Our choise for iterative solver has been the transpose free quasi minimal residual method (TFQMR) [2], which is efficient, handles non-symmetric and non-Hermitian matrices well, and even manages to solve nearly singular matrices.

1) Numerical evaluation of operators: The operators in our problem generally involve derivatives and spatial functions appearing in multiplicative form. We discretize the equations by treating the derivatives in Fourier domain and the spatial functions in real domain. To perform the calculations we Fourier transform the trial vectors back and forth from spatial domain to spectral domain and vice versa. This is justified because derivation in Fourier domain, and multiplication by a function, i.e., ε, in real domain are both $O(N)$ operations for a trial vector with N elements. The prohibitive factor is the FFT, which is an $O(N\ln(N))$ operation. Alternatively, we could operate exclusively in Fourier domain, by treating multiplications by ε by means of discrete convolution, which is a costly $O(N^3)$ operation.

We illustrate the aforementioned ideas by an example: The application of the operation $\partial_x\{1/(j\omega\varepsilon(x,y))\}\partial_y$ to a trial vector $\mathbf{f}$ consists of the following steps:

- multiply $\mathbf{f}$ by a $y-$derivative matrix, to be defined below,
- inverse Fourier transform the result,

- multiply the result by a sampled version of $1/(j\omega\varepsilon(x,y))$,
- Fourier transform, and, finally,
- perform the $x-$derivative.

The computation of derivatives is fairly straightforward. Once the reciprocal lattice vectors k_1 and k_2 have been chosen, differentiation with respect to $x-$coordinates yields multiplication by a diagonal matrix with elements being

$$j[(\widehat{m}+K_1)k_1^x+(\widehat{n}+K_2)k_2^x], \quad m\in[0,M-1], n\in[0,N-1], \tag{28}$$

where K_1 and K_2 are Bloch phasing factors and k_1^x and k_2^x are projections of reciprocal lattice vectors on the $x-$axis. The whole number $\widehat{m}$ is defined as follows

$$\widehat{m}=\begin{cases} m & 0\le m\le \frac{M}{2} \\ m-M & \frac{M}{2}<m\le M-1 \end{cases}. \tag{29}$$

A similar definition holds for $\widehat{n}$. The rational behind this definition is that we need to include negative harmonics into the set of basis functions in order to make it complete. The ordering of harmonics is irrelevant, however, this choice is implemented in most FFT algorithms. The matrix for the $y-$derivative can be obtained from (28) by replacing the projections on $x-$axis with projections on $y-$axis.

2) Solving excitation problems: The interface condition for the magnetic field can be written as follows

$$\lim_{\delta\to 0} h_x\left(z^0+\frac{\delta}{2}\right)-h_x\left(z^0-\frac{\delta}{2}\right)=\rho_y(z^0), \tag{30}$$

where $h_x(z)$ is the $x-$directional magnetic field component and ρ_y is a $y-$directional current element. Consider (19b) and insert a new layer, designated by h'_{o+1}, at the location $z=(o+1)\Delta-\delta$ where δ represents an infinitesimally small distance.

Assume that there is a horizontal current filament ρ positioned at plane $z=(o+1)\Delta-\frac{\delta}{2}$. Using the above information and (30) we can rewrite (19b) in order to include the assumed excitation,

$$\mathbf{h}_o-\mathbf{h}_{o+1}+\mathbf{B}'_{o+\frac{1}{2}}\mathbf{e}_{o+\frac{1}{2}}=-\rho_{o+\frac{1}{2}}. \tag{31}$$

We specify the excitation by $o+\frac{1}{2}$ since it is inserted between the layers o and $o+1$. The incorporation of this condition into the system equation (21) can be achieved by simply replacing the RHS zero vector by the Fourier transform of the assumed excitation current function

$$\mathbf{M}_\mathbf{K}(\omega)\mathbf{f}_\mathbf{K}(\omega)=\rho_\mathbf{K}(\omega). \tag{32}$$

The Bloch vector $\mathbf{K}$ and angular frequency ω are written explicitly in (32) to emphasize their role as input parameters.

It should be pointed out that using the Bloch-wave basis not only we can solve phased-periodic excitation problems, but also we can tackle elementary excitation problems: The latter are defined as elementary non-periodic excitations of geometrically periodic structures.

3) Solving eigenproblems: Equation (21) is a homogeneous system and has non trivial solutions if and only if $\mathbf{M}$ is singular. Therefore, the eigenmodes of the system for a given $\mathbf{K}$ can be found by defining a suitable measure for the detection of the singularity of $\mathbf{M}$ as a function of ω. A possible measure for singularity is, e.g. the magnitude of the determinant. However, solving determinants iteratively is computationally costly and complicated. Instead, we propose a method which is more physics-based: We assume a current distribution to excite the system under consideration, and compute the square norm of the resulting field coefficients. For $\mathbf{M}$ near the singularity, the norm grows - ideally - without bounds. Furthermore, the solution approaches the eigenvector corresponding to the eigenvalue 0. The formal justification for this approach is given in [3] but we review the important steps here:

Consider the following system of equations

$$\mathbf{A}\mathbf{y}=\mathbf{b}. \tag{33}$$

Both sides of this equation can be expanded in terms of the eigenvectors $\mathbf{v_j}$ of $\mathbf{A}$ as

$$\sum_j \alpha_j\lambda_j\mathbf{v_j}=\sum_\mathbf{j}\beta_\mathbf{j}\mathbf{v_j}. \tag{34}$$

Here α_j is the coefficient set for $\mathbf{y}$ and λ_j is the eigenvalue of $\mathbf{A}$ corresponding to eigenvector $\mathbf{v_j}$. Due to the linear independence of the eigenvectors, we can write

$$\mathbf{y}=\sum_j\frac{\beta_j}{\lambda_j}\mathbf{v}_j. \tag{35}$$

From this form it is easy to see that if one of the eigenvalues λ_j is close to zero, the only significant contribution to the solution comes from the corresponding eigenvector $\mathbf{v}_j$. Furthermore, as λ_j approaches zero, the norm of the solution vector approaches infinity.

This behaviour can be understood from physical reasoning as well: If the system is in resonance with the excitation, the energy in the system grows indefinitely as time elapses rendering the eigensolution an infinite energy.

Instead of seeking the maximum of the solution norm, we alternatively, seek the minimum of its inverse

$$G_\mathbf{K}(\omega)=\frac{1}{\sqrt{||\mathbf{f}_\mathbf{K}(\omega)||_2}}, \tag{36}$$

where $\mathbf{f_K}$ is the solution to (32). The introduction of the square root is to smoothen out the curve. We have a great flexibility in choosing the current distribution for eigenmode computations but practise has shown that with a few randomly placed and oriented dipoles the functional G behaves smoothly between the singular points. One should be aware of the fact if $<\mathbf{v}_j,\mathbf{b}>=0$ in (33), then $\beta_j=0$ and the solution norm does not grow even if $\lambda_j=0$. As an example, this happens if the system is excited with a single $y-$directional dipole positioned exactly at a node of h_x for the corresponding eigenmode. Numerically this means that G does not necessarily possess a minimum even if $\mathbf{M}$ is singular for a given ω.

4) Preconditioning: Typically, iterative solvers converge poorly for non-preconditioned systems, and very often they even completely fail to converge. Therefore, the implementation of a good preconditioner is a prerequisite for performance enhancement. Instead of solving (32), we suggest solving the modified system in (37)

$$\mathbf{P}_1^{-1}\mathbf{M}\mathbf{P}_2^{-1}\left(\mathbf{P}_2\mathbf{f}\right)=\mathbf{P}_1^{-1}\rho, \tag{37}$$

for the new unknown vector $\mathbf{y}=\mathbf{P}_2\mathbf{f}$. The problem is to find suitable preconditioner matrices $\mathbf{P}_1$ and $\mathbf{P}_2$ such that the solver converges faster for the new matrix $\mathbf{B}=\mathbf{P}_1^{-1}\mathbf{M}\mathbf{P}_2^{-1}$. It can be shown that the convergence is quicker if $\mathbf{B}$ is near diagonal.

We construct $\mathbf{P}_1$ out of submatrices which we encounter in the main block diagonal of the matrix $\mathbf{M}$. More precisely, we discretize the matrix operator elements $\mathscr{A}_{\infty,\infty}$, $\mathscr{A}_{\in,\in}$, $\mathscr{B}_{\infty,\infty}$ and $\mathscr{B}_{\in,\in}$ defined in (10) and (12) for all $z-$layers in the system, from which we can construct a block diagonal matrix. In place of boundary condition matrices in $\mathbf{M}$, we use diagonal unity matrices in $\mathbf{P}_1$. Due to the block diagonal property, $\mathbf{P}_1$ is fairly easy to invert, as each block can be inverted individually. However, it should be noted that in practice $\mathbf{P}_1$ is never actually constructed nor inverted: Instead we first invert the operators analytically in a sense that $\mathscr{L}^{-1}\left(\mathscr{L}f\right)=f$ for a suitably chosen test function f, and then carry out their discretized versions as outlined earlier. As an example, the inverse of $\partial_x\left\{1/\left(j\omega\varepsilon_o(x,y)\right)\right\}\partial_y$ is $\mathbf{I}_y\left(j\omega\varepsilon_o(x,y)\right)\mathbf{I}_x$ where $\mathbf{I}_\xi$ denotes integration with respect to ξ. In Fourier domain, integrals can be computed by the application of the inverse of the derivative matrix (28).

It should be noted that (28) may contain zero elements and, therefore, prevent inversion. However, there is a simple remedy to circumvent this problem: *select a suitable orientation for the lattice vector relative to the coordinate system*. We illustrate this idea with an example. However, before doing so, we summarize a few facts from the theory of Fourier analysis which will be of help to our discussion.

Comments:

- **Invariance and symmetry properties of the Fourier transform:** A significant part of the utility of the Fourier transform is due to the fact that it has natural invariance properties under the actions of rotations, dilations, and translations. In particular, a rotation is an orthogonal matrix with determinant 1 (a special orthogonal matrix).

- **Proposition:** Let ρ be a rotation of $\mathbf{R}^N$. We define $\rho f(x)=f(\rho(x))$. Then we have the formula: $\widehat{\rho f}=\rho\widehat{f}$

  Proof: Remember that ρ is orthogonal and has determinant 1. We then have

$$\widehat{\rho f}(\xi)=\int dt\,(\rho f)(t)e^{-jt\xi} \tag{38a}$$
$$=\int dt\,f\left(\rho(t)\right)e^{-jt\xi} \tag{38b}$$
$$=\int ds f(s)e^{-j\rho^{-1}(s)\xi} \tag{38c}$$
$$=\int ds f(s)e^{-js\rho(\xi)} \tag{38d}$$
$$=\widehat{f}(\rho\xi) \tag{38e}$$
$$=\rho\widehat{f}(\xi). \tag{38f}$$

  In the above we have used the variable substitution $s=\rho(t)$, and the fact that $\rho^{-1}=\rho^T$ for an orthogonal matrix, with the superscript T denoting the transposition.

We now are in a position to continue with our example. Consider a rectangular lattice with reciprocal lattice vectors $\mathbf{k}_1=k_1\mathbf{u}_x$ and $\mathbf{k}_2=k_2\mathbf{u}_y$. The projections of $\mathbf{k}_1$ and $\mathbf{k}_2$, respectively, onto the $x-$axis are $k_{1,x}=k_1$ and $k_{2,x}=0$. Assuming for the components of the Bloch phasing factor $K_1=0$ and $K_2\neq 0$ results in a zero element in (28) for $\widehat{m}=0$. A simple yet very effective solution to this problem can be obtained by rotating the original $(x,y)-$coordinate system around the $z-$axis about an angle θ. Denote the new coordinate system by $(\tilde{x},\tilde{y},\tilde{z})$. Projections of $\mathbf{k}_1$ and $\mathbf{k}_2$, respectively, onto the $\tilde{x}-$axis are $k_{1,\tilde{x}}=k_1\cos(-\theta)$ and $k_{2,\tilde{x}}=k_2\cos(\pi/2-\theta)\neq 0$. The angle θ can easily be selected in such a manner that there are no zero elements in either of the derivative matrices. The solution to the problem remains unaltered as the choice of the coordinate system is arbitrary.

It should be noted that there is still the point $[K_1,K_2]=[0,0]$ at which the singularity cannot be removed by changing the coordinate system. (The point $\mathbf{K}=\mathbf{0}$ corresponds to strictly periodic field distributions without any phase change

in two consecutive cells. The field is static and no wave propagation takes place.) Therefore, $\mathbf{K} = \mathbf{0}$ does not cause a serious problem: All bounded fields in the slab have $\omega = 0$ at this point.

Additional improvements can be achieved by appropriately choosing the matrix $\mathbf{P}_2$. Our approach is to use the system matrix for a simpler auxiliary problem for which $\partial_x \varepsilon(x,y,z) = \partial_y \varepsilon(x,y,z) \equiv 0$, and, $\overline{\varepsilon}_k = \text{ave}(\varepsilon_k(x,y))$ where ave means averaging in the $(x,y)-$plane over one unit cell. Since $\overline{\varepsilon}_k$ is constant in our auxiliary problem, the resulting system matrix $\widehat{\mathbf{M}}$ will have nonzero elements only on five diagonals. This matrix can be constructed explicitly. Our goal is that $\mathbf{P}_2^{-1}$ diagonalizes $\mathbf{P}_1^{-1}\mathbf{M}$ as closely as possible. Therefore, we set

$$\mathbf{P}_2 = \text{diag}(\mathbf{P}_1^{-1})\widehat{\mathbf{M}}, \tag{39}$$

where ''diag (**A**)'' means the main diagonal of **A**. Instead of explicitly inverting $\mathbf{P}_2$ we perform an LU-decomposition and use the resulting coefficients to solve $\mathbf{x} = \mathbf{P}_2\mathbf{f}$. In our implementation of the LU-decomposition we omit pivoting. This omission enables us to store the coefficients in locations of nonzero elements of the original matrix, instead of occupying a general banded matrix. Fortunately, it appears as if pivoting is not necessary in first place: In our systematic and comprehensive testings we never encountered a vanishingly small pivot element.

In summary, the application of $\mathbf{P}_1^{-1}\mathbf{M}\mathbf{P}_2^{-1}$ to a certain test vector $\widetilde{\mathbf{f}}$ consists of the following steps: *i*) Compute $\mathbf{z} = \mathbf{P}_2^{-1}\widetilde{\mathbf{f}}$ by solving $\widetilde{\mathbf{f}} = \mathbf{P}_2\mathbf{z}$ using the LU-coefficients, *ii*) compute $\mathbf{x} = \mathbf{M}\mathbf{z}$, and, finally, *iii*) apply $\mathbf{P}_1^{-1}$ to $\mathbf{x}$. Once the iterative solver reports convergence, the non-preconditioned solution can be obtained from $\mathbf{f} = \mathbf{P}_2^{-1}\widetilde{\mathbf{f}}$.

We conclude this section with the following remarks: *i*) Setting $\mathbf{P}_1 = \mathbf{I}$ and $\mathbf{P}_2 = \widehat{\mathbf{M}}$ is sufficient to solve the system. However, defining $\mathbf{P}_1$ as described above seems to improve the iterative procedure by a significant factor in most problems and not worsen it in any problems we have solved so far. *ii*) We also experimented with a diagonal preconditioner in which $\mathbf{P}_1 = \mathbf{I}$ and $\mathbf{P}_2 = \text{diag}(\mathbf{M})$. However, the results were not satisfying. For most problems the system did not converge at all, and even if it did, thousands of iterations were required. *iii*) Typically, convergence requires $10-300$ iterations, depending on the specific values of $\mathbf{K}$ and ω, and the function $\varepsilon(x,y,z)$, and the singularity of $\mathbf{M}$.

III. Numerical Results

We have computed a variety of test examples with our method and compared them, whenever possible, to the corresponding results obtained by the planewave method [4].

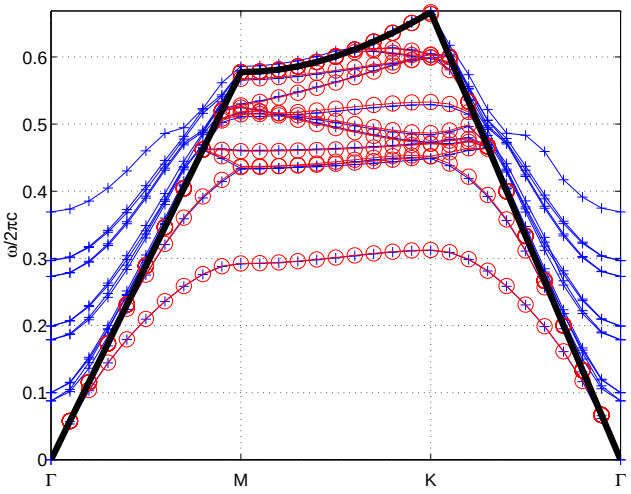

Fig. 1. Shows the dispersion diagram for a triangular lattice of cylindrical holes (voids) in a dielectric slab. Curves marked with 'o' have been computed with our method, and those marked with with '+' have been computed with the planewave method. The thick black line represents the light-line along which the modes become guided in free space. Modes located above this line are not guided by the slab, and are artifacts due to artificial periodization of the structure required by the planewave method.

Planewave method is not fully adapted to slab problems, because it assumes the structure to be periodic in all spatial directions. It can be used though, by introducing a long lattice vector in $z-$direction. This extended unit cell, a supercell, is first filled with the background material and the slab is then inserted into it. This approach is justified as long as the modes of interest are well confined around the slab in $z-$direction, and thus the interaction between neighbouring supercells can be assumed to be negligibly small. If the modes are not well localized, the solutions will interfere, and we can expect a significant deterioration of the results. Furthermore, modes that are not guided by the slab, will appear guided due to this artificial periodization. Results can be verified by increasing the $z-$directional lattice vector until convergence is reached.

A. Dispersion diagram of equilateral triangular lattices

Our first test case is an equilateral triangular lattice of cylindrical air holes (voids) in a dielectric slab. The thickness of the slab is $h_z = 0.4$, and the dielectric constant is $\varepsilon = 12$. The radius of the air holes is $r = 0.38$, and the lattice constant $a = 1.0$. The cladding material above and below the slab is free space.

Dispersion diagram computed with our method and with the planewave method is shown in Fig. (1).

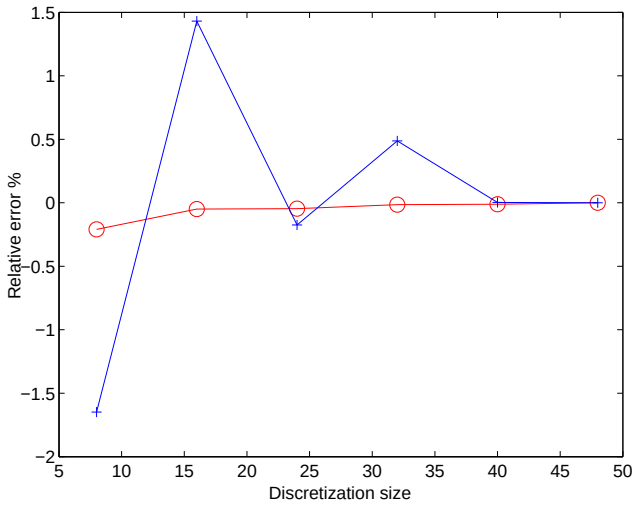

Fig. 2. Convergence as a function of grid size for the lowest order mode at $\mathbf{K} = [0, 0.5]$. Relative error compared to the result obtained with 48 grid points in all directions. The curve with marker '+' is computed with the planewave method, while the curve with marker 'o' with our method. It can be seen that our method provides accurate results with comparatively few grid points. The difference between the two methods at finest discretization is 0.0205%

In both methods we used 32 planewaves in both lattice vector directions. In our method, we used 25 electric field layers and 24 magnetic field layers in $z-$direction. In the planewave method we used a super-cell with the periodicity length in $z-$ direction being $10a$, with a denoting the lattice constant. Thereby, we employed 384 planewaves. This results in 15.36 planewaves for a slab with the thickness $h_z = 0.4$.

Quite often the lowest bands are the most significant ones; therefore, we conducted a convergence analysis for the first mode at the $M-$point ($\mathbf{K} = [0, 0.5]$) (see Fig. (1)). We solved the problem utilizing both methods with several discretizations and compared the results as shown in Fig. (2). Problem parameters were as above except that we used the same number of grid points in all directions. In the planewave method this means using $10/0.4 = 25$ times more planewaves in $z-$direction in order to compensate for the larger super-cell size.

B. *Fields in an array of dielectric spheres*

Our second test case consists of a rectangular lattice of dielectric spheres positioned on a dielectric substrate. The structure is shown in Fig. (3).

The fields shown in Figs. (4) and (5) are solved for the lowest order eigenmode, at the frequency $\omega = 0.298(2\pi c)$

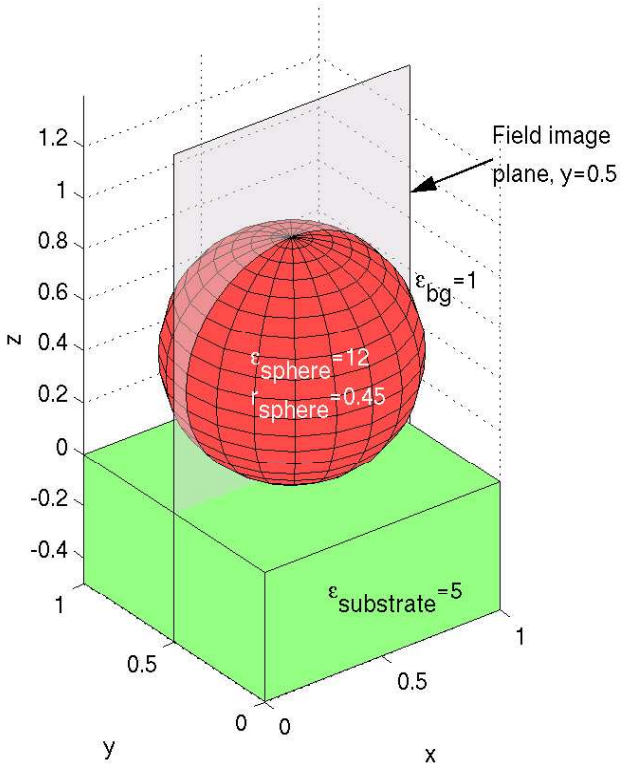

Fig. 3. Geometry of test case 2. Spheres with $r = 0.45$ are positioned on a dielectric substrate with a rectangular lattice specified by $a = 1$. The spheres, having the dielectric constant $\varepsilon_{sphere} = 12$, are immersed in free space. The dielectric constant of the substrate is $\varepsilon_{substrate} = 5$. Fields are plotted on the plane marked with $y = 0.5$.

and the point $[K_1, K_2] = [0.5, 0.5]$. The eigenfrequency has been determined iteratively using the technique described in Section 3); when the result converged, we Fourier transformed the solution to get the real space fields.

In the solution we used 48 planewaves in $x-$direction, and 48 planewaves in $y-$direction. In $z-$direction we used 48 and 47 layers for the electric and magnetic fields, respectively. The electromagnetic field outside the slab ($z < 0$ and $z > 0.9$) has been computed using the eigenpairs for Maxwell's equations in free space. Note that we already have constructed these eigenpairs for the implementation of boundary conditions. Note also that having imposed the interface- and boundary conditions the unknowns in our problem, and, therefore, field distributions in the slab as well as in free space are uniquely determined. Finally, note that while the transversal fields e_1, e_2, h_1 and h_2 have been obtained from the solution of (37), the orthogonal field components e_3 and h_3 are computed as a postprocessing step using (14).

IV. Acknowledgements

One of the authors (K. Varis) thanks the Finnish Graduate School of Modern Optics and Photonics, and the Ausseninstitute at Vienna University of Technology for providing research scholarships which made possible a visit to Vienna, Austria for finalizing the current project.

This work was partially done while the second author (A. R. Baghai-Wadji) was visiting the Institute for Mathematical Sciences, National University of Singapore and Institute for High Performance Computing (IHPC) in 2003. This visit was supported by the Institute and IHPC.

References

[1] K. Varis, and A. R. Baghai-Wadji, ''A Novel 2D Pseudo-spectral Analysis of Photonic Crystals,'' submitted for publication (ACES Journal 2004).

[2] R. W. Freund, N. M. Nachtigal, ''A Transpose-Free Quasi-Minimal Residual Algorithm for Non-Hermitian Linear Systems,'' SIAM Journal on Scientific Computing. 14 (1993) pp. 470-482

[3] W. H. Press, S. A. Teukolsky, W. T. Wetterling, and B. P. Flannery, ''Numerical Recipes in C: the Art of Scientific Computing,'', Cambridge University Press, Cambridge, pp. 493-495, 2nd edition, 2002.

[4] S. G. Johnson, and J. D. Joannopoulos, ''Block-Iterative Frequency-domain Methods for Maxwell's Equations in a Planewave Basis,'' Optics Express 8, no., 173-190, 2001.

Karri Varis was born in Espoo, Finland, in 1974. He received a M.Sc. degree in Electrical Engineering from Helsinki University of Technology in 1999. Since then, he has been a doctoral student in the Finnish Graduate School of Modern Optics and Photonics

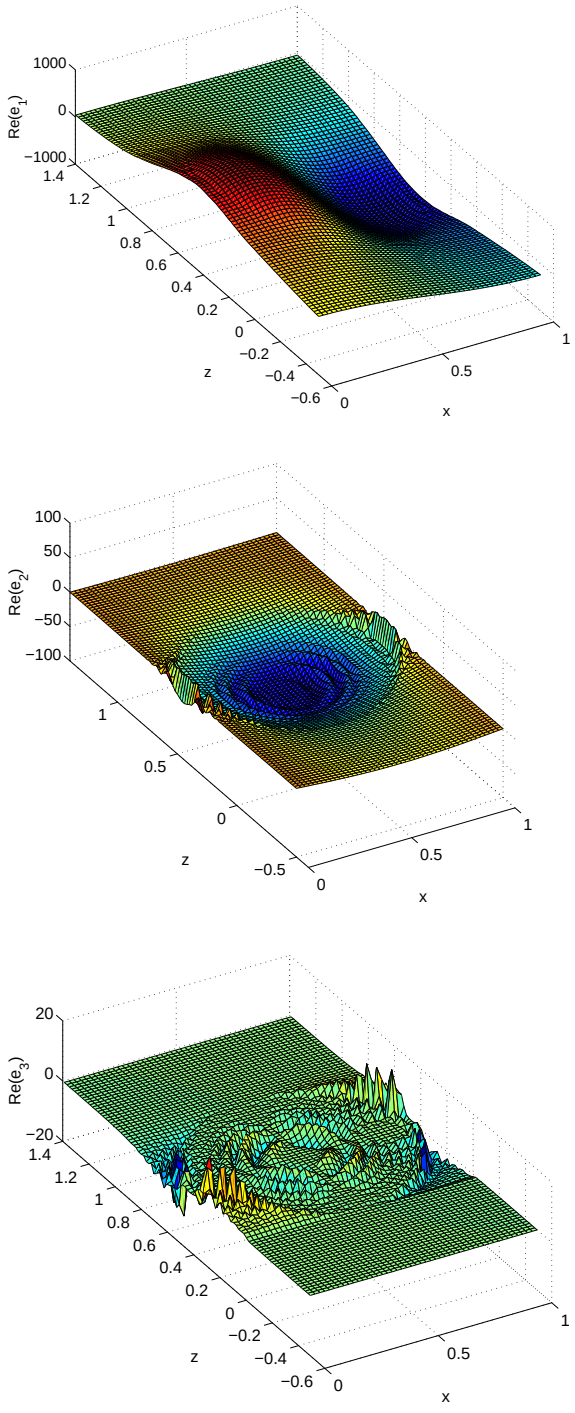

Fig. 4. Electrical field distributions for test case 2, which consists of dielectric spheres on a dielectric surface. Spheres are centered at $[x, y, z] = [0.5, 0.5, 0.45]$ and for $z < 0$ the dielectric constant is $\varepsilon_{subst} = 5$. The spheres are immersed in free space. Ripples on e_3 are most likely due the properties of Fourier transform. However, the amplitude of this field component is negligibly small.

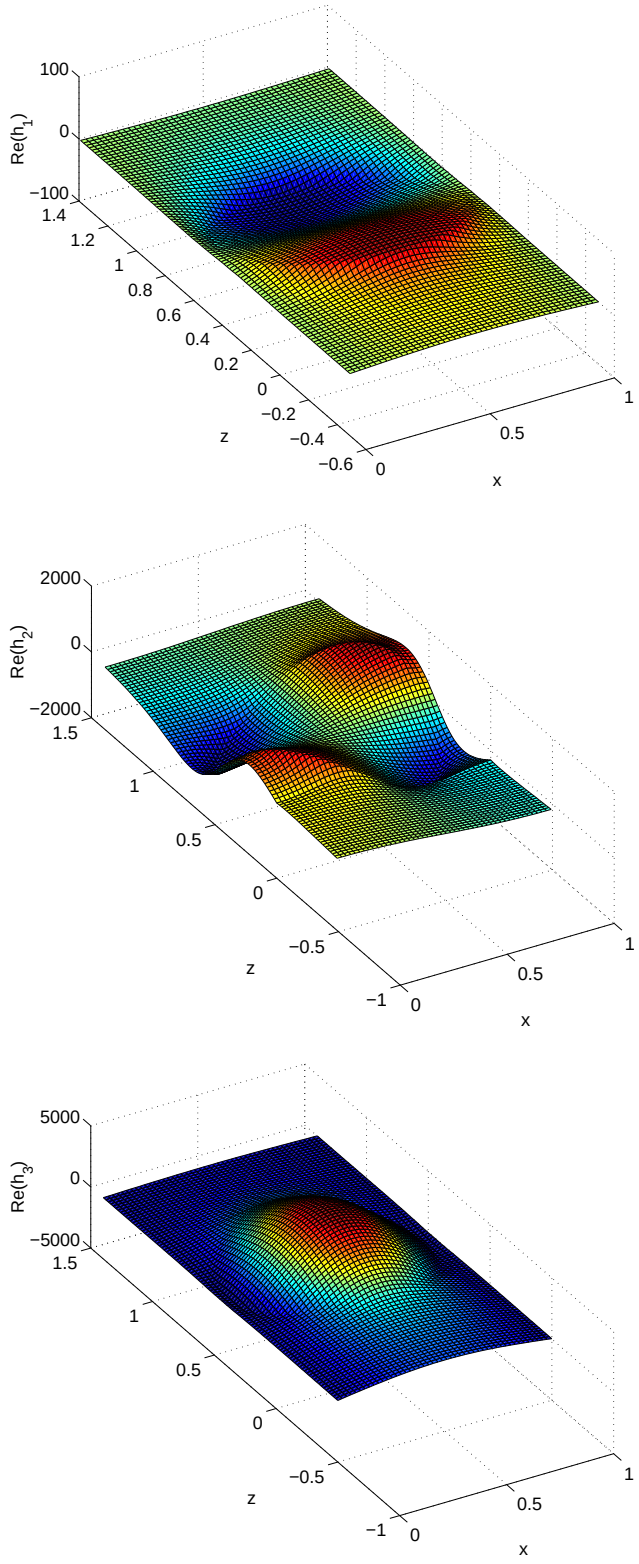

Fig. 5. Magnetic fields for testcase 2.

and working in the Optoelectronics Laboratory, Helsinki University of Technology. His current research interest includes the enhancement and development of computational techniques for the analysis of periodic and non-periodic systems, with an emphasis on photonic crystals and optical devices.

Ali R. Baghai-Wadji was born in Marand, Iran, on May 6, 1953. He has been with the Electrical Engineering and Information Technology Department at Vienna University of Technology (VUT), Vienna, Austria, since 1979. From 1979 to 1984 he was an associate researcher in Physical Electronics and Applied Electronics Groups, where he developed computer models for microelectronic and microacoustic devices. He earned his M.Sc. and Ph.D. in electrical engineering in 1984 and 1987, respectively, and obtained his *venia docendi* in physical electronics in 1994, all from VUT. Since 1997 he has been an associate professor at VUT. Currently he is heading the Accelerated Computational Technology (ACT) Group at the Institute for Fundamental and Theory of Electrical Engineering at VUT. Three times he was awarded the Kurt Gödel research scholarship from Austria, allowing him to spend a total of 10 months at UCI, University of California, Irvine, during the years 1990, 1991, and 1992. From 1994 to 1999 he was, on leave of absence from VUT, a principal engineer consultant in the United States serving more than four years for Motorola, Government System and Technology Group, Scottsdale, Arizona, and nearly one year for CTS-Wireless components in Albuquerque, New Mexico. In 1999 and 2000 he was (15 months) a visiting professor at Materials Science Laboratory, Helsinki University of Technology (HUT). That professorship was awarded by Nokia Research Foundation, and TEKES, a national science foundation in Finland. In addition, in the Fall 2000 he was awarded a Nokia Visiting Fellowship. In 2003 he was awarded a *venia docendi* for modeling and simulation of classical and quantum electronic devices and materials at HUT for an initial period of 6 six years. In 2003 he was four months an invited senior member of the Institute for Mathematical Sciences, and a visiting professor at the Institute for High Performance Computing, in Singapore. Since 1995 he has also been affiliated with Arizona State University as an adjunct professor at the Department for Mathematics and Statistics. In 2002 he was elected an honorary member of the Electromagnetics Academy, Massachusetts, USA. He has supervised five PhD dissertations, and eleven Masters' theses. He has lectured 12 short courses at various IEEE conferences internationally. He has authored more than 120 publications in reviewed journals and conference proceedings, and has one patent. His current research interest includes the development of accelerated computational modeling techniques, quantum mechanics, photonic crystals, and molecular electronics. Since 1995 he has been a senior member of the IEEE, an IEEE-UFFC associate editor, and an IEEE-UFFC technical program committee member. He was the guest editor for a special issue on *Modeling, Optimization, and Design of Surface and Bulk Acoustic Wave Devices* in IEEE Transactions on Ultrasonics, Ferroelectrics, and Frequency Control (Sept. 2001, Vol. 48, Num. 5). He will serve as the general chairman of the PIERS'05 conference.